Flow-based Rate Maximization for Link Aggregation Enabled Hybrid LiFi-WiFi Network

Saswati Paramita, *Graduate Student Member, IEEE,* Arani Bhattacharya, *Member, IEEE,* Rizwana Ahmad, *Graduate Student Member, IEEE,* Vivek Ashok Bohara, *Senior Member, IEEE,* and Anand Srivastava, *Member, IEEE*

***Abstract*—Light Fidelity (LiFi) is one of the most promising techniques to meet such high demand for indoor users by utilizing the visible light spectrum. A major challenge of LiFi is that its coverage is relatively limited, as the surrounding walls, objects, and other surfaces mostly absorb visible light. Thus, a number of studies have proposed aggregating the bandwidth of WiFi and LiFi to serve all users within a room. However, complementing LiFi with WiFi via bandwidth aggregation typically comes with an overhead in terms of both aggregation and computation, which reduces the data rates that can be used. Furthermore, data provided to users are often also limited by the backhaul capacity, which is typically wired Ethernet in indoor settings. In this work, we model the utilization of the functioning of WiFi and LiFi access points as a two-dimensional flow graph and show that the problem of maximizing the sum of data rate across all users is NP-Hard in practice. We then design an algorithm FLADA to solve this problem by solving its relaxed version where the variables are treated as real numbers, and then rounding to the nearest integer. We prove formally that it provides a solution that is at least $0.5\times$ the optimal. We further compare it with a greedy baseline approach through extensive simulations and show that it outperforms it by up to 81.6%.**

***Index Terms*—LiFi, WiFi, Aggregation, Linear programming, Hybrid LiFi-WiFi Network, Link aggregation overhead.**

I. Introduction

The last few years have witnessed a considerable increase in demand for higher data rates from wireless devices, especially in indoor communication scenarios. This has put an additional burden on wireless networks, predominantly using radio frequency (RF) to facilitate communication among users and access points (APs). This may precipitate the scenario of 'spectrum crunch' or the unavailability of the RF spectrum by 2035 [1]. Thus, researchers are exploring extended parts of the electromagnetic spectrum, such as visible light (VL), which can be one of the possible alternatives to the RF spectrum. Light Fidelity (LiFi) is one of the most promising such alternatives that are currently being explored [2]. Unlike its WiFi counterpart, light fidelity (LiFi) employs the VL spectrum for indoor communication. Specifically, LiFi utilizes light-emitting diodes (LEDs) for illumination and communication by exploiting existing illumination infrastructure. Moreover, LiFi has additional advantages as it can offer high data rates in the Gbps range due to the availability of a massive unregulated spectrum [3]. Furthermore, it is inherently secure as lights cannot penetrate the walls, has no health hazards, and has minimal interference with other electromagnetic (EM) devices. Thus, the utilization of LiFi has a lot of promise for emerging applications such as augmented reality (AR) and virtual reality (VR), which demand large bandwidth.

Saswati Paramita, Vivek Ashok Bohara and Anand Srivastava are with Wirocomm Research Group, IIIT-Delhi. Arani Bhattacharya is with the Department of Computer Science and Engineering, IIIT-Delhi. Rizwana Ahmad is with University of Cambridge (E-mail: saswatip@iiitd.ac.in, arani@iiitd.ac.in, ra714@cam.ac.uk, vivek.b@iiitd.ac.in, anand@iiitd.ac.in).

Utilizing LiFi, however, has some challenges, as it is significantly affected by blockages and has confined coverage areas due to the strong directional nature of light. Therefore, the data rates provided by LiFi fall significantly if the users are present in the 'blind spots', i.e., locations where the intensity of the signal is low. To circumvent this limitation, prior studies have suggested the utilization of LiFi/WiFi heterogeneous network [4]. In such a network, LiFi is complemented with WiFi so that LiFi offers a higher data rate in a confined coverage area, whereas WiFi provides a moderate data rate with extensive coverage for indoor users. Further, LiFi and WiFi operate at different frequencies; hence they do not interfere with each other. In a conventional heterogeneous (HetNet) network, users can receive data from either LiFi or WiFi AP. However, in such a network, users at the edge of blind spots or having small amounts of movement would require frequent handovers from LiFi to WiFi APs or vice-versa [5].

A possible technique of reducing number of handovers in heterogeneous networks is link aggregation (LA). In link aggregation-enabled LiFi and WiFi HetNet (LA-HLWN), as shown in Fig. 1, users receive data concurrently from LiFi and WiFi APs [6]. Therefore, the data rate can be enhanced by fulfilling user satisfaction with fewer handovers from LiFi to WiFi. However, since WiFi's signals travel physically farther than that of a LiFi AP, the WiFi APs would get overloaded unless user data rate demands are intelligently allocated. Thus, AP selection and allocation of data rate need to be done efficiently to avoid unnecessarily overloading WiFi APs.

Prior works that have looked at the problem of intelligent allocation in LA-HLWN have primarily utilized deep reinforcement learning [7], [8]. Furthermore, they utilize simplified models of subcarrier allocation in modern WiFi and LiFi systems, without considering the constraints used by the new WiFi standards while utilizing OFDMA [9]. While such techniques provide high data rates to users, they come with the overhead of long convergence times and high computation complexity [10]. Since the controller used by HLWN has limited compute capability, we argue for the need to have a less compute-intensive technique of data rate allocation.

A second challenge of utilizing LiFi comes from connec-

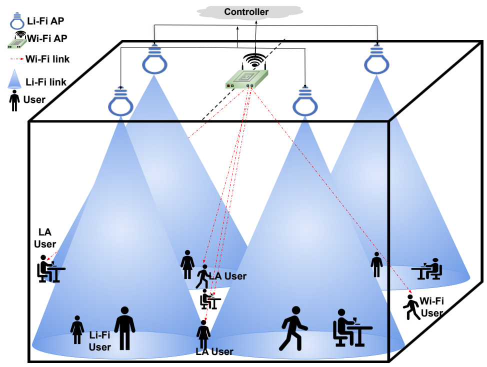

Fig. 1: An illustration of realistic LA-enabled hybrid LiFi and WiFi network. A user at the edge of LiFi AP coverage region tends to utilize both WiFi and LiFi.

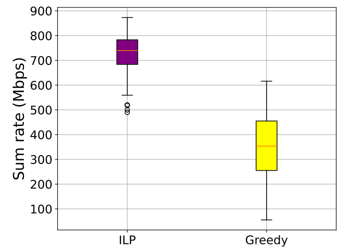

Fig. 2: Comparison of the sum rate obtained in two distinct cases of hybrid LiFi-WiFi network – aggregation with an optimal case of ILP, aggregation with greedy algorithm.

tivity with the network core. Traditional WiFi usually used Ethernet protocol to carry data to the network core. While most LiFi deployments available today utilize Ethernet, this often reaches capacity of the underlying Ethernet backhaul [11]. Current studies on network aggregation, however, do not consider the limitations of the backhaul and limit their study to efficient aggregation.

In this paper, we formulate the allocation of user data rates as a multi-dimensional commodity flow problem [12], [13], [14]. Our formulation takes into account the data rates demanded by the user, the quality of the signal to each AP, the condition of the backhaul networks of each AP, and the constraints inherent in LA-HLWN networks as well as the requirement of fair data rates. We show that this problem is NP-Hard [15], and thus cannot be solved optimally in polynomial time. We, therefore, propose an algorithm FLADA (Flow-based Algorithm for Data rate Allocation) that first formulates it as an integer linear programming (ILP) and then solves its relaxed version as a linear programming problem (LPP). We apply rounding on the solution given by the LPP, which leads to the release of some data rates. These released data rates are reallocated as much as possible without violating the fairness constraints. We formally prove that the result obtained gives at least 0.5 times the optimal result (see Theorem 3 of Section IV.C for details).

Our simulation setup considers an indoor scenario for analysis, as shown in Fig. 1. We have evaluated the performance of the LA-enabled heterogeneous LiFi-WiFi network for our proposed algorithm FLADA using various performance metrics such as sum rate, average rate, contributions of APs for the user's achieved rate, user satisfaction, Jain's fairness, time complexity, and energy efficiency. The evaluation in Section V shows that our proposed algorithm FLADA provides 82% of the optimal data rates given by an optimal ILP approach in a single room with 4 LiFi APs and 1 WiFi AP. Furthermore, it also outperforms a baseline greedy approach by 56% and the basic LPP version without additional reallocations (referred to as Base-FLADA) by 31% in the above scenario.

A. Motivation

Our primary motivation is to maximize data rates allocated to the users in link aggregation-enabled heterogeneous LiFi-WiFi networks. To motivate this using a single case study (details of the setting is discussed in Section VI), we show the improvement in the sum rate for link aggregated LiFi-WiFi networks in Fig. 2. The sum rate is defined as the sum of all users' achieved data rate for a specified network and a specified number of users. The most straightforward strategy, greedy, allocates APs to users by identifying the one that provides the highest data rate. We observe that utilizing the greedy algorithm to allocate data rates leads to a significant fall in the total allocation of around 50%. Data rates using aggregation may fall because aggregation comes with some additional overhead due to channel heterogeneity [16]. This shows that a more intelligent algorithm to allocate data rates is essential to ensure high allocation.

However, assigning APs to users to maximize the data rates is non-trivial. An optimal approach, typically solved using an integer linear programming solver, often takes on average over $10s$ on even a desktop machine, making it unsuitable for use (details in Section V). Thus, an algorithm that runs fast in practice while also providing high data rates is essential.

B. Summary of Contributions

We summarize our major contributions as follows:

- We formulate the problem of AP selection and rate maximization for an LA-enabled HLWN as a flow graph.
- We design an algorithm, FLADA that utilizes LPP rounding and reallocation that guarantees a data rate of at least 0.5 times the optimal for the proposed model.
- We evaluate the proposed system for multiple simulation settings under different fairness constraints to show that the proposed system outperforms the baseline greedy by up to 81.6% for tight fairness and 56% for moderate fairness case. We also show that link aggregation of LiFi with WiFi provides a significantly higher data rate compared to the case of no link aggregation.

II. Related Work

We classify related works into three categories – heterogeneous LiFi/WiFi networks but without aggregation, aggregation-enabled heterogeneous LiFi/WiFi networks, and link aggregation in other networks.

Heterogeneous LiFi/WiFi Networks Without Aggregation: Multiple studies have proposed solutions to alleviate the problem of spectrum scarcity owing to the limited availability of RF spectrum. For instance, [17], [18], [19], [6] alleviate the above problem of limited availability of RF spectrum by using heterogeneous LiFi/WiFi system. In a heterogeneous LiFi/WiFi system, the user receives the data from either LiFi or WiFi based on the received signal strength (RSS) at a particular location. In [17], the authors have provided a dynamic load-balancing scheme to mitigate the problem of overload on WiFi AP due to the mobility of the users. The quasi-static users are connected to LiFi, and the mobile users get connected to WiFi. The authors have also considered the utility function, which deals with fairness and throughput. X.Li et al. have proposed centralized as well as distributed load balancing algorithms in [18] for cooperative load balancing in a hybrid RF/VLC system. The authors have analyzed both throughput and fairness in scenarios having diverse cell formations. The work [19] discussed the difference between homogeneous and heterogeneous networks and proposed a two-stage AP selection algorithm. They developed a fuzzy logic system for heterogeneous LiFi/WiFi network in the first stage. The remaining users are assigned to a homogeneous LiFi network in the second stage. This paper compared the proposed method with optimization methods, such as the max-sum-log-rate to show that it improves throughput than conventional methods and also achieves a close-to-optimal throughput with lower complexity. The work [6] investigated the benefits of energy efficiency for heterogeneous LiFi/WiFi systems. They formulated an optimization problem of maximizing energy efficiency with the constraints of power and bandwidth allocations.

The above works discussed about heterogeneous LiFi/WiFi network performance without link aggregation. Alternatively, the following works have focused on the performance improvement of the heterogeneous LiFi/WiFi network with link aggregation (LA).

Link-Aggregation Enabled Heterogeneous LiFi/WiFi Networks: Only a few works on heterogeneous LiFi/WiFi networks have explored link aggregation. The authors in [5], [20], [21], [22],[23], [24], and [25] have explored various layers of the protocol stacks for LA-enabled heterogeneous LiFi-WiFi network. Fan Jin et al. in [5] have proposed a decentralized algorithm to solve the sub-optimal problem of network selection and resource allocation for multimode and multihome mobile terminals. Multihome MTs are able to aggregate the resources from different networks, whereas multimode MTs are able to select single networks. The authors have evaluated and compared the performance of both multihome and multimode MTs based on delay requirements. However, these works have focused on RSS-based user association to demonstrate the advantage of LA without optimizing the data rates. The work [26] uses Lyupanov optimization to ensure that the required data rates are achieved while balancing the energy consumption among visible light and RF waves. In [20], authors have provided the proof of concept of link aggregation of LiFi and WiFi in a LA enabled HLWN. The authors in [21] have focused on the demonstration of link aggregation, which considers multiple access, mobility, handover, and multipath transmission control protocol. In [22] and [25], the authors have implemented and demonstrated link aggregation at the physical layer using IEEE 802.11ac-supported WiFi interface. Further, the authors in [23] have implemented link aggregation at the data link layer using the Linux operating system's bonding driver. Y.S.M. Pratama et al. in [24] have used the Lyapunov optimization function to achieve desired throughput in a bandwidth-aggregated RF-VLC system. However, none of these works consider the constraints of the user's demand, location, capacity, fairness, and AP's backhaul capacity for optimal data rate allocation.

On the other hand, Yang, Helin, et al. in [27] focused on energy-efficient resource management problem, which deals with joint network selection, sub-channel assignment, and power management to meet the required transmission reliability and latency. They have proposed a reinforcement-based learning algorithm to manage the resources intelligently in heterogeneous industrial networks. Further, in [7], the authors have proposed a complex reinforcement learning-based algorithm to solve the problem of load balancing in heterogeneous LiFi-WiFi networks. In [28], J. Kong et al. explored the power allocation problem by proposing a Q-learning-based algorithm. However, these works do not provide performance guarantees and require extensive training data for bootstrapping.

All these works do not consider the overhead due to link aggregation. Moreover, the trade-off between fairness and user satisfaction has also not been addressed for LA-enabled LiFi-WiFi Hetnets. Although our previous work [29] considers the overhead, it relies on exhaustive search to allocate resources, which is computational as well as time intensive and may be difficult to implement in realistic scenarios.

Flow-based Optimization of Multipath Transmission: In [30], authors have formulated a joint optimization problem of resource allocation and transmission coordination for the heterogeneous network of macro and pico base stations. They use the a flow-based framework as a tool to evaluate the performance of the network. Wang et al. [31] have focused on optimizing user association, subchannel, and power allocation jointly for a multicell multi-association orthogonal frequency division multiple access (OFDMA) heterogeneous networks for downlink transmissions in long-term evolution. The authors have solved this optimization problem in two steps: (a) optimized the user association and subchannel allocation for fixed power allocation using graph theory, (b) optimized power allocation for fixed user association and subchannel allocation by using the Karush-Kuhn-Tucker conditions and approximation algorithm. In [32], the authors have proposed a belief propagation (BP) algorithm to optimize user association, subchannel assignment, and power allocation jointly for heterogeneous cellular networks using a factor graph model. In [33], the authors have minimized the resources used with respect to user association in three-tier HetNets using a distributed algorithm that used 1D and 2D search. These works are not directly applicable to our scenario, as they do not consider the type of resource unit allocations performed by WiFi or LiFi networks. Furthermore, cellular networks have much better backhaul capacities [34] than indoor networks, as in indoor networks the wired ethernet serves as the backhaul.

TABLE I: Symbols and variables with their descriptions

Symbol	Description
r_i^0	data rate allocated to user i
r_i^1	number of APs allocated to user i
g_{wi}^0	data rate allocated to user i over WiFi channel
g_{wi}^1	number of WiFi APs utilized by user i (either 1 or 0)
g_{li}^0	data rate allocated to user i over LiFi channel
g_{li}^1	number of LiFi APs utilized by user i (either 1 or 0)
h_{ij}^0	data rate allocated to user i over j^{th} AP
h_{ij}^1	whether user i utilizes j^{th} AP
u_{ij}	resource units utilized by user i over j^{th} AP
b_j	data rate utilized of j^{th} AP across all users
R_i	demand required by user i's application
H_{ij}	channel capacity of user i from j^{th} AP per RU
U_j	number of RUs available in j^{th} AP
B_j	backhaul capacity of j^{th} AP
β	link aggregation overhead
γ	constraint on user satisfaction
m	total number of users
n	total number of WiFi APs
p	total number of LiFi APs
s	user application, serving as the source node of the graph
t	Internet, serving as the sink node of the graph

Thus, these works cannot be directly used for our purpose. Our work builds on these strategies to model the problem in the context of heterogeneous LiFi/WiFi network.

III. System model and design

A. Description of the System

We consider a system with m number of users, n WiFi APs, and p LiFi APs for an indoor scenario of known dimensions. The APs are mounted on the room's ceiling, and a set of users are present in the room. A central controller (CC) connected to all the APs, assigns APs to each user based on their individual demand and channel conditions. The demand R_i of i^{th} user is the maximum data rate that a user requires, and it depends on applications which varies among the users. For example, a video with a maximum resolution of 1080p is known to have a maximum data rate of $7.4 Mbps$.

The user may be given either part or its entire data rate demand. We denote the data rate available to the user i by r_i^0. Each user can be connected to at most one LiFi AP, one WiFi AP, or both. If both the APs are used by a single user, we then say that the user is using *link aggregation*.

The data rate r_i^0 allocated to a user is limited by its demand R_i as well as the total bandwidth allocated. As in modern WiFi standards IEEE 802.11ax and IEEE 802.11be (WiFi 6 and 7), we assume OFDMA is used to allocate bandwidth to each user. The bandwidth can be allocated in pre-specified resource units (RU) as specified in the IEEE 802.11be (WiFi 7) standard [9]. In this standard, a bandwidth of 20 MHz can be split into 9 smaller RUs of 2 MHz, 4 smaller RUs of 4 MHz, 2 smaller RUs of 8 MHz or 20 MHz utilized together. Each of these RUs has its own modulation and coding scheme (MCS) ranging from binary phase-shift keying to 4096-Quadrature Amplitude Modulation (4096-QAM), as allowed by the standard. A single user receives a maximum data rate equal to the product of the number of RUs allocated, the amount of bandwidth per RU, and the spectral efficiency of the MCS, which is a known constant. In case blockages are present, we assume the probability of a particular user facing a blockage is known, and we consider the expected bandwidth. For convenience, we denote the product of the amount of bandwidth per RU and the spectral efficiency of the MCS by H_{ij}.

We denote the data rate used by user i from the AP j by h_{ij}^0. We assume that the total number of resource units available at j^{th} AP is equal to U_j. For notational convenience, we assume that the WiFi APs are numbered from 1 to n, whereas the LiFi APs are numbered from $n+1$ to $n+p$. Note that although for LiFi APs, OFDMA has been proposed by multiple research works, it is not yet part of the standard. We assume a similar mechanism of splitting RU's as in WiFi APs, as the LiFi standards borrow most of the channel allocation mechanisms from the WiFi standards.

In case a user utilizes link aggregation, then there is reordering of packets, which consumes some additional overhead, leading to reduction of throughput. We quantify this overhead as $1-\beta$ where $0 \leqslant \beta \leqslant 1$, i.e., $(1-\beta)$ times the sum of data rates is lost due to reordering of packets. Thus, if a user receives data from both LiFi and WiFi APs, its data rate r_i^0 is also limited to $\beta \times (g_{wi}^0 + g_{li}^0)$". Based on the values considered in literature [8], [29], an average link aggregation overhead value of 0.2, i.e., β = 0.8 has been considered.

Each AP also has a backhaul that connects it to the core network. Each such backhaul has a bandwidth capacity, depending on the AP's own capability and the type of wired network used for the backhaul. Since this network is usually stable, we consider this to be a constant denoted by B_j for each AP j.

The goal of the above system is to maximize the sum of the data rates allocated to each user. However, this is also subject to fairness constraints, where a few users should not get more allocated data rates at the cost of other users. We model this by adding a parameter called fairness coefficient, denoted by γ. The minimum data rate allocated to the user must exceed γ times the highest data rate allocated.

B. Our Graph Model

We visualize this entire system as a flow graph shown in Fig. 3. The flow graph consists of five layers of nodes:

1) The source node s, which represents overall user requirements according to the applications.
2) A node corresponding to each user, denoted by f_i.
3) Each f_i has one node representing the utilization of WiFi or LiFi AP each, denoted by f_i^w and f_i^l, respectively.
4) Each WiFi AP and LiFi AP has one corresponding node, denoted by a_j where $j = 1, 2, ..., n$ and $j = n+1, n+2, ..., n+p$ for WiFi and LiFi, respectively.
5) The destination node t, representing the Internet.

The numbers above the edges in Fig. 3 denote their flow capacities. The first dimension of the flow capacities represents whether the amount of data available for use. The second dimension of the flow capacities represents a limit on the number of possible connections. Thus, since each user can only connect to a total of two APs, but can utilize data rates up to their demand, the capacity of an $< s, f_i >$ edge is

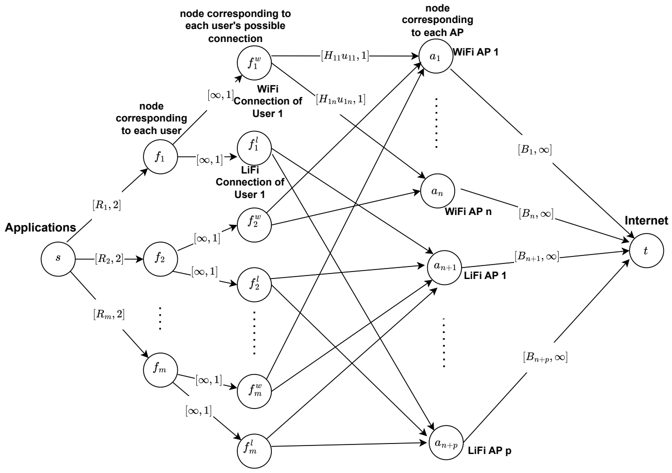

Fig. 3: A flow graph denoting the capacities and the node labels. The nodes f_i represent the user device, the nodes f_i^w denote the requirements filled by WiFi, the nodes f_i^l denote the requirements filled by LiFi, the nodes a_j represent the requirements supported by WiFi APs for j = 1, 2, ..., n whereas the nodes represent the data rates supported by LiFi APs for j = n+1, n+2, ..., n+p.

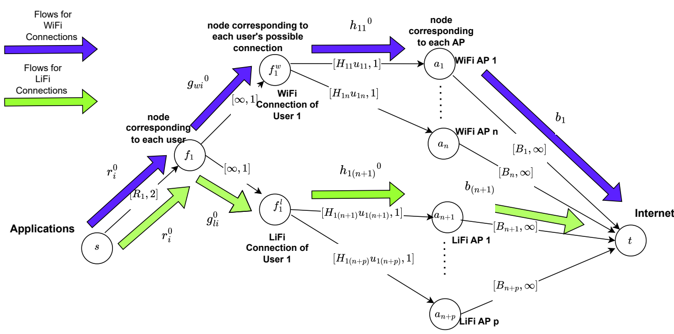

Fig. 4: Two specific flows are depicted on the flow graph. The blue and green arrows represent data rates over the WiFi and LiFi channels respectively.

$[R_i, 2]$. Similarly, since a user can use only one WiFi and one LiFi AP, and data is not constrained by the type of AP, the capacities of $< f_i, f_i^w >$ and $< f_i, f_i^l >$ are equal to $[\infty, 1]$.

An example of data rates obtained (flows) by a specific user is shown in Fig. 4, with the blue and green lines denoting the data rates over WiFi and LiFi channels respectively. Note that the first-dimensional flow is correlated with the second-dimensional flows, as without a connection from a user to an AP, the user cannot use the corresponding channels. Having visualized the problem in the form of a flow graph, we now formulate it formally.

IV. Problem formulation & Solution

We now formulate the above problem as a mixed integer-linear programming problem (MILP). Our goal is to select the data rates r_i^q, h_{ij}^q and b_j, $\forall i = 1, \ldots, m, j = 1, \ldots, n+p, q = \{0, 1\}$. This corresponds to a multi-dimensional flow maximization problem, which can be formally solved as an instance of integer linear programming. The goal is to maximize the total data rates given to the user, i.e.

$$\textbf{Maximize} \sum_{i=1}^{m} r_i^0. \tag{1}$$

We now formally define the constraints. A basic feature of this problem is that for any intermediate node (i.e. all nodes except s and t), the flows are conserved. Intuitively, this is because any data cannot be stored by either the user devices or the APs. Formally,

$$r_i^q = g_{wi}^q + g_{li}^q, \forall i = 1, \ldots, m, \forall q = \{0, 1\}, \tag{2}$$

$$g_{wi}^q = \sum_{j=1}^{n} h_{ij}^q, \forall i = 1, \ldots, m, \forall q = \{0, 1\}, \tag{3}$$

$$g_{li}^q = \sum_{j=n+1}^{n+p} h_{ij}^q, \forall i = 1, \ldots, m, \forall q = \{0, 1\}, \tag{4}$$

$$\sum_{i=0}^{m} h_{ij}^0 = b_j, \forall j = 1, \ldots, n+p. \tag{5}$$

Our next constraints are the capacity constraints on all the flows. These constraints depend on the type of edge. We enumerate each of them along with a brief explanation:

$$r_i^0 \leqslant R_i, \forall i = 1, \ldots, m, \text{i.e,}$$
$$\text{(each user gets data rate at most equal to demand)} \tag{6}$$

$$h_{ij}^0 \leqslant H_{ij} u_{ij}, \forall i = 1, \ldots, m, \forall j = 1, \ldots, n+p,$$
$$\text{(each user gets data rate not more than the product of capacity of RU and number of RU's allocated)} \tag{7}$$

$$b_j \leqslant B_j, \forall j = 1, \ldots, n+p, \text{ and}$$
$$\text{(the data rate of each AP is limited by its backhaul capacity)} \tag{8}$$

$$r_i^1 \leqslant 2, \forall i = 1, \ldots, m, \text{i.e.}$$
$$\text{(no user can connect to more than two APs)} \tag{9}$$

We also have constraints that specify that an AP can be used to provide data rate if and only if a user connects to it. We formalize this for both WiFi and LiFi APs as follows:

$$h_{ij}^1 > \lceil u_{ij}/U_j \rceil \tag{10}$$

We also consider the overhead of aggregation by setting an additional constraint on the data given to a user u_i. This constraint is activated only if both WiFi and LiFi APs are used. Formally,

$$r_i^0 \leqslant \beta g_{wi}^0 + \beta g_{li}^0 + M(1 - g_{wi}^1) + M(1 - g_{li}^1), \tag{11}$$

where M is a large constant with a value higher than all the flows. We formalize the fairness constraints for APs using a relaxed form of max-min fairness, where the minimum rate allocated to user i must not be lower than γ times of the maximum allocated rate to any other user in the system:

$$r_i^0 \geqslant \gamma r_j^0, \forall i, j \in \{1, \ldots, m\} \tag{12}$$

The bandwidth constraints on WiFi and LiFi APs are:

$$\sum_{i=1}^{m} u_{ij} \leqslant U_j, \forall j \in \{1, \ldots, n+p\} \tag{13}$$

Also, we note that all the variables denoting data rates r_i^0, g_{wi}^0, g_{li}^0, h_{ij}^0, b_j are real numbers, i.e:

$$r_i^0, g_{wi}^0, g_{li}^0, h_{ij}^0, b_j \in \mathbb{R}, \forall i = 1, \dots, m, j = 1, \dots, n+p$$

The variables denoting individual AP allocation g_{wi}^1, g_{li}^1, h_{ij}^1 are binary integers, i.e:

$$g_{wi}^1, g_{li}^1, h_{ij}^1 \in \{0,1\}, \forall i = 1, \dots, m, j = 1, \dots, n+p$$

The variable denoting number of APs allocated to each user can be an integer from 0 to 2, i.e:

$$r_i^1 \in \{0,1,2\}, \forall i = 1, \dots, m$$

The number of RUs allocated u_{ij} can be any non-negative integer, i.e.

$$u_{ij} \in \mathbb{Z}_{\geqslant 0}, \forall i = 1, \dots, m, j = 1, \dots, n+p.$$

Expressions (1)–(13) together represent a well-defined mixed integer linear programming (MILP) problem. We call this as the 2-dimensional mixed max-flow (2DMMF) problem. Solving it would provide the connections for each pair of user and AP, such that the total user demand is satisfied. However, solving an MILP is an NP-Hard problem that takes exponential time, and so it is not feasible to run it fast enough in practice. Furthermore, we prove by a reduction in the following theorem that the above-defined flow problem is NP-Hard.

Theorem 1. *The 2DMMF Problem is NP-Hard.*

Proof. We prove this by showing that a particular instance of the above problem is the 0-1 multiple knapsack problem. Assume that we have only LiFi APs, i.e., $n = 0$. Furthermore, let $R_i = \infty$, $B_j = \infty$ and $\gamma = 0$. Each LiFi AP has a total of U_j RUs. Thus, each user has to be allocated an integral number of RU's from specific APs. We write this as:

$$\textbf{Maximize} \sum_{i=1}^{m} \sum_{j=0}^{p} H_{ij} u_{ij}, \tag{14}$$

subject to the constraints:

$$\sum_{i=1}^{m} u_{ij} \leqslant U_j, \forall j = 1, \dots, p, u_{ij} \text{ is an integer, and} \tag{15}$$

$$\sum_{j=1}^{p} \lceil u_{ij}/U_j \rceil \leqslant 1, \forall i = 1, \dots, m. \tag{16}$$

The above problem is identical to the 0-1 multiple knapsack problem, indicating that our problem is NP-Hard. □

Since this problem is NP-Hard, it is not feasible to get an optimal solution in polynomial time. While it is possible to utilize integer linear programming to obtain an optimal solution, the amount of time taken to allocate channels is unacceptably high (as discussed in Section I.A). We, therefore, design an approximate algorithm to solve the problem.

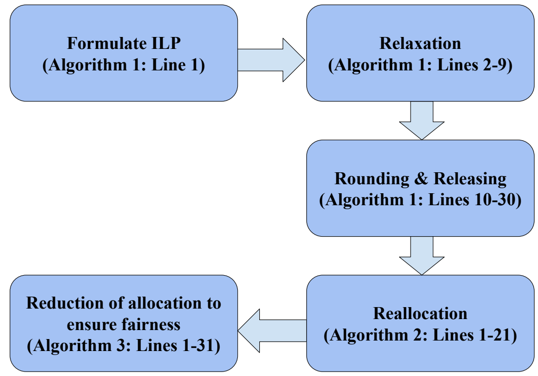

Fig. 5: Flow chart detailing the steps of FLADA.

Algorithm 1 Generation of feasible result using LPP solver and rounding

INPUT: $R_i, H_{ij}^0, B_j, \forall i = 1, \dots, m, j = 1, \dots, n+p,$
OUTPUT: Values $r_i^q, h_{ij}^q, b_j, \forall i = 1, \dots, m, j = 1, \dots, n+p, q = \{0,1\},$

1: Formulate the ILP as described in Expressions (1)–(12)
2: Use LPP solver to solve the relaxed version of ILP
3: **for all** $i \in [1, \dots, m]$ **do**
4: $a_w \leftarrow \text{argmax}_{j=1}^{n} h_{ij}^0$
5: $a_l \leftarrow \text{argmax}_{j=n+1}^{n+p} h_{ij}^0$
6: $h_{ij}^q \leftarrow 0, u_{ij} = 0, \forall j = n, \dots, n+p, j \notin \{a_l, a_w\}, \forall q \in \{0,1\}$
7: $g_{wi}^0 = h_{ij}^0, j = a_w$
8: $g_{li}^0 = h_{ij}^0, j = a_l$
9: **end for**
10: **for all** $i \in [1, \dots, m]$ **do**
11: **if** $r_i^1 = 2$ **then**
12: /* Release WiFi AP if overhead is higher than WiFi rate alone */
13: **if** $[g_{wi}^0 + g_{li}^0] \times \beta < g_{li}^0$ **then**
14: $a_w \leftarrow \text{argmax}_{j=1}^{n} g_{wi}^0$
15: $b_j \leftarrow b_j - g_{wi}^0, j = a_w$
16: $u_{ij} \leftarrow 0, j = a_w$
17: $g_{wi}^q \leftarrow 0, \forall q \in \{0,1\}$
18: $r_i^0 \leftarrow g_{li}^0$
19: $r_i^1 \leftarrow 1$
20: /* Release LiFi AP if overhead is higher than LiFi rate alone */
21: **else if** $[g_{wi}^0 + g_{li}^0] \times \beta < g_{wi}^0$ **then**
22: $a_l \leftarrow \text{argmax}_{j=n}^{n+p} g_{li}^0$
23: $b_j \leftarrow b_j - g_{li}^0, j = a_l$
24: $u_{ij} \leftarrow 0, j = a_l$
25: $g_{li}^q \leftarrow 0, \forall q \in \{0,1\}$
26: $r_i^0 \leftarrow g_{wi}^0$
27: $r_i^1 \leftarrow 1$
28: **end if**
29: **end if**
30: **end for**
31: **return** r, g, h, u, b

V. Our Solution Approach

Our solution approach FLADA as shown in Fig. 5 consists of five steps. The first step, shown in Algorithm 1 includes using an LPP solver and rounding. We relax the MILP into a linear programming problem. Thus, we relax all the integer values to real numbers, and solve the linear programming problem (Line 2). We then use a rounding algorithm to convert them back into integers and then compute the actual flows. The rounding algorithm (Lines 3-9) checks for each user the AP that provides the highest data rate separately for both LiFi and WiFi. The data rates from the other APs are all set to 0, as users can utilize only one among WiFi and LiFi. After that, for

Algorithm 2 Reallocation to increase the data rate.

INPUT: $R_i, H^0_{ij}, B_j, \forall i = 1, \ldots, m, j = 1, \ldots, n+p,$
OUTPUT: Values $r^q_i, h^q_{ij}, b_j, \forall i = 1, \ldots, m, j = 1, \ldots, n+p, q = \{0, 1\},$

1: **for all** $[1, \ldots, m]$ **do**
2: $L \leftarrow$ sorted users in ascending order of $R_i - r^0_i$
3: $a \leftarrow \max_{i=1}^{m} R_i - r^0_i$
4: $i \leftarrow L[0]$
5: $a_w = \max_{j=1}^{n} h^0_{ij}$
6: $a_l \leftarrow \max_{j=n+1}^{n+p} h^0_{ij}$
7: **if** $a_w > 0$ **then**
8: $j = a_w$
9: $v_{ij} \leftarrow \min(R_i - r^i_0, H_{ij}U_{ij} - h^0_{ij}, B_j - b_j, a/\gamma)$
10: $h^0_{ij} \leftarrow v_{ij} + h^0_{ij}$
11: $g^0_{wi} \leftarrow v_{ij} + g^0_{wi}$
12: $b_j \leftarrow v_{ij} + b_j$
13: **end if**
14: **if** $a_l > 0$ **then**
15: $j \leftarrow a_l$
16: $v_{ij} \leftarrow \min(R_i - r^0_i, H_{ij}U_{ij} - h^0_{ij}, B_j - b_j, a/\gamma)$
17: $h^0_{ij} \leftarrow v_{ij} + h^0_{ij}$
18: $g^0_{li} \leftarrow v_{ij} + g^0_{li}$
19: $b_j \leftarrow v_{ij} + b_j$
20: **end if**
21: **end for**
22: **return** r

Algorithm 3 Release of data rates to satisfy fairness constraint.

INPUT: $R_i, H^0_{ij}, B_j, \forall i = 1, \ldots, m, j = 1, \ldots, n+p,$
OUTPUT: Values $r^q_i, h^q_{ij}, b_j, \forall i = 1, \ldots, m, j = 1, \ldots, n+p, q = \{0, 1\},$

1: $L \leftarrow$ sorted users in descending order of $R_i - r^0_i$
2: **for all** $i \in L$ **do**
3: $b' \leftarrow r^0_i - a/\gamma$
4: /*Reduce allocation to u_i by b' */
5: **if** $b' < 0$ **then**
6: **return** r
7: **end if**
8: /*Reduce WiFi allocation by w_r to x_{ij}*/
9: $x_{ij} \leftarrow \min(b', g^0_{wi})$
10: $r^0_i \leftarrow r^0_i - x_{ij}$
11: $g^0_{wi} \leftarrow g^0_{wi} - x_{ij}$
12: **for all** $j \in [1, \ldots, n]$ **do**
13: **if** $h^0_{ij} > 0$ **then**
14: $v_{ij} \leftarrow \max(0, h^0_{ij} - x_{ij})$
15: $h^0_{ij} \leftarrow v$
16: $b_j \leftarrow b_j - v$
17: $x_{ij} \leftarrow x_{ij} - v$
18: $r^0_i \leftarrow r^0_i - v$
19: **end if**
20: **end for**
21: /*Reduce LiFi allocation by x_{ij} to u_i*/
22: $x_{ij} \leftarrow b' - w_r$
23: $g^0_{li} \leftarrow g^0_{li} - x_{ij}$
24: **for all** $j \in [n+1, \ldots, n+p]$ **do**
25: **if** $r^0_{ij} > x_{ij}$ **then**
26: $g^0_{li} \leftarrow \max(0, g^0_{li} - x_{ij})$
27: $b_j \leftarrow b_j - x_{ij}$
28: $r^0_i \leftarrow r^0_i - x_{ij}$
29: **end if**
30: **end for**
31: **end for**
32: **return** r

LiFi and WiFi it checks whether using aggregation provides higher data rate than any one of them individually (Lines 10-30). If so, then it retains the connections to both LiFi and WiFi without making any changes. Otherwise, it retains the connection only to the AP that provides the maximum.

Utilizing Algorithm 1, however, leads to a substantial amount of unutilized capacity. This is because the capacity released during the rounding process is not allocated. Thus, we introduce our second step of reallocation, shown in Algorithm 2. Algorithm 2 observes the association with the APs, and sorts the users in the descending order of their remaining demands of data rates. It then identifies the allocation of data rates that could be added without exceeding any among the demand of the user, the channel capacity and the backhaul capacity. It adds this allocation and then goes to the next user to repeat this process.

Running Algorithm 2 could lead to the fairness constraint being violated. Thus, we utilize Algorithm 3 to reduce the allocation for a user violating the fairness constraint by the amount necessary to satisfy it. Note that a higher value of γ imposes stricter fairness, and thus it would reduce the allocation by a higher amount (Line 3 of Algorithm 3). Once this computation is complete, it then releases the resources used from both WiFi and LiFi channels and backhaul capacities. Finally, it returns the flows r.

A. *Performance Bounds of FLADA*

We now prove the performance guarantee of FLADA. Our proof relies on the fact that FLADA uses an LP solver, which is known to give optimal solution to the assignment problem. We then show that the LP rounding technique only leads to a reduction of data rate of half the total allocated, and thus gives us an approximation ratio of 0.5.

Lemma 1. *Given a fixed flow into f^w_i's and f^l_i's, the allocation given by the LP is optimal.*

Proof. We note that identifying the optimal WiFi APs and allocating their data rates is equivalent to the 2-dimensional assignment problem. Similar is the case for identifying the optimal LiFi APs. Note that 2-dimensional assignment problems get optimal results by solving an LPP. Since Algorithm 1 also allocates APs by solving LPP, our technique also ensures optimal allocation of the data rates through WiFi and LiFi APs given the values sent over WiFi and LiFi APs are fixed. □

Theorem 2. *LP-Rounding followed by running Algorithms 2–3 provides a feasible solution to the 2DMMF Problem.*

Proof. We note that the LP-rounding technique allocates between 1-2 APs to each user (according to Expressions (6)–(8)). The LP-rounding also satisfies all the capacity, demand and backhaul constraints. However, after rounding and releasing, the data rate allocated to the least user may reduce. Note that reallocation can only add additional allocation (preferably to the user with the lowest allocation), but does not guarantee satisfaction of the fairness constraint. Thus, Algorithm 3 checks if the fairness constraint (given by Expression (12)) is violated and if so, it reduces the allocation from the users who have received the highest data rates by a value that satisfies the fairness constraint. Thus, all the constraints are satisfied by the solution eventually given by Algorithm 3, and so our solution is feasible.

□

Lemma 2. *The solution given by Algorithm 1 provides a constant-factor approximation that is at least* 0.5 *times the optimal, i.e.*

$$O_r \geqslant 0.5O^*, \tag{17}$$

where O_r *and* O^* *denote the sum of data rates assigned by our approach and the ILP respectively.*

Proof. We first consider the relaxed version of the 2DMMF problem obtained by LP-Rounding. Let the solution returned by this problem be O_{LPP}. We denote the optimal solution, returned by the ILP, by $O*$. Then, since the LPP has weaker constraints but identical objective, we have:

$$O_{LPP} \geqslant O^*. \tag{18}$$

We now consider the solution obtained after rounding and releasing (Lines 10-30 of Algorithm 1). This step reduces the amount of data rate allocated. We now show that the amount of allocation can only be reduced to half of O_{LPP}. To see this, we note that from each node corresponding to each user f_i, there are only two outgoing edges from f_i. Thus, the lowest value of g^0_{wi} or g^0_{li} is set to 0, which retains at least a data rate of $\max(g^0_{wi}, g^0_{li})$. We note that:

$$\max(g^0_{wi}, g^0_{li}) \geqslant (g^0_{wi} + g^0_{li}) \times 0.5. \tag{19}$$

Summing on both sides over the users, we get:

$$\sum_{i=1}^{m} \max(g^0_{wi}, g^0_{li}) \geqslant \sum_{i=1}^{m} (g^0_{wi} + g^0_{li}) \times 0.5. \tag{20}$$

Note that the expression on LHS above gives us the flow received after rounding O_r. The expression on RHS is equal to half the total flow given by the LPP. Thus, we get:

$$O_r \geqslant 0.5O_{LPP}. \tag{21}$$

Now, from the inequalities (18) and (21), we get Eqn. (17). □

Lemma 3. *The amount of reduction of data allocated from a user to an AP in Algorithm 3 never exceeds the data added in Algorithm 2, i.e.* $x_{ij} \leqslant v_{ij}\ \forall i = 1, \dots, m, j = 1, \dots, n+p$.

Proof. From Line 9 of Algorithm 2, we have: $v_{ij} \leqslant b/\gamma$, where b is the flow of the user which has minimally satisfied. From Lines 4 and 8 of Algorithm 3, b' is the amount of reduction necessary to achieve fairness. Now, note that $b' \leqslant b$, since the amount of reduction must be smaller than the flow of the least user. This implies that the total amount of reduction in Algorithm 3 is less than the amount of flow added in Algorithm 2. □

Lemmas 2-3 now clearly show that the total sum rate after running Algorithms 1-3 satisfy the following result:

Theorem 3. *The sum rate obtained after running Algorithms 1-3 is at least* 0.5 *times the optimal sum rate.*

B. Time Complexity

To find out the time complexity, we first compute the total number of variables by counting the total number of edges in the flow graph as:

1) A total of m edges from s to node corresponding to each user f_i's.
2) A total of $2m$ edges from node corresponding to each user f_i to node corresponding to each user's possible connection f^w_i and f^l_i.
3) A total of $m(n+p)$ edges from all the f^w_i's to node corresponding to each AP a_j's for $j = 1, 2, ..., n+p$.
4) A total of $n+p$ edges from all the a_j's to t for $j = 1, 2, ..., n+p$.

The total number of edges is, therefore, equal to $3m + mn + mp + n + p$. This gives us a total of $2 \times (3m + mn + mp + n + p)$ variables. Since solving LPP takes $O(v^3)$ time complexity, where v is the number of variables, this gives us a time complexity of $O(m^3(n^3+p^3)$ in solving the LPP. For the rounding, our algorithm iterates over all the users, and then computes the AP that gives the maximum. This takes $O(mn + mp)$ time. Similarly, reallocation also iterates over all users and APs, taking $O(mn + mp)$ time. Thus, the time complexity is dominated by the LPP solver, giving us a total time complexity of $O(m^3(n^3 + p^3))$. Since the number of users is limited to 30, the number of WiFi APs is smaller than the number of LiFi APs (which is in turn usually smaller than 15 in a room), so the overall problem is easily tractable and solvable in a few milliseconds. Note that directly solving the ILP takes $O(2^{mn+mp})$, which in practice takes more than a second to run. This makes it impractical to use.

VI. Performance Evaluation and Discussion

A. Simulation settings

We consider an indoor environment of $5 \times 5 \times 3m^3$ room, as shown in Fig. 1. Four LiFi APs are installed on the four quadrants of the ceiling, and a single WiFi AP is at the center of the ceiling. However, the WiFi AP provides full coverage compared to a single LiFi AP in this room dimension. The four LiFi APs are placed to get the coverage area of approximately $3m^2$ to $4m^2$ with some LiFi attocell overlapping. Thus, the user can receive the data from LiFi and WiFi APs concurrently using the link aggregation technique. Furthermore, we define $\zeta^{LiFi}_{i,k}$ is signal-to-interference noise ratio (SINR) received at the user from LiFi AP and is modelled as [19]:

$$\zeta^{LiFi}_{ij} = \frac{\left(\mathbf{R}_{PD} I^{LiFi}_{ij} P_{opt}/\mathbf{K}\right)^2}{N_{LiFi}U_{ij} + \sum_{\substack{l_\alpha \in l_j \\ \alpha \neq j}} \left(\mathbf{R}_{PD} I^{LiFi}_{ij} P_{opt}/\mathbf{K}\right)^2}. \tag{22}$$

Here, $\mathbf{R}_{PD}$ is the responsivity of the PD, $\mathbf{K}$ is the coefficient of optical to electrical power conversion, P_{opt} is the transmitted power from LiFi AP. N_{LiFi} is defined as the power spectral density (PSD) of noise. Also, the LiFi channel impulse response is expressed as [19]:

$$I^{LiFi}_{ij} = \frac{(L_m+1)A_{PD}}{2\pi d^2_{ij}} \cos^l(\Theta_{ij}) \cos(\Phi_{ij})\, g_c(\Phi_{ij})\, g_f. \tag{23}$$

TABLE II: LiFi and WiFi channel parameters [6], [29]

LiFi channel parameters	
Height of the AP from user level (h)	2.15 m
PD's Area (A_{PD})	1 cm^2
Optical filter's gain (g_{f})	1
PD's FOV	90°
Optical to electric conversion efficiency ($\mathbf{K}$)	3
Responsivity of the detector ($\mathbf{R}_{PD}$)	0.53 A/W
LiFi AP's optical transmit power (P_{opt})	3 Watts
Fixed power consumption of LiFi AP (P_{LiFi})	4 Watts
LiFi AP's bandwidth (U_{ij})	40 MHz
LiFi noise PSD (N_{LiFi})	-210 dBm/MHz
WiFi channel parameters	
Central carrier frequency (f_{c})	2.4 GHz
Transmit Power of WiFi AP (P_{WiFi})	20 dBm
Power consumption in WiFi AP (P_{w})	6.7 Watts
Bandwidth of WiFi AP (U_{ij})	20 MHz
WiFi noise PSD (N_{WiFi})	-75 dBm/MHz

In (23), $d_{i,j}$ is the euclidean distance between the AP j and user i. The $\Theta_{i,j}$ and $\Phi_{i,j}$ are irradiance and incidence angles, respectively, A_{PD} is the physical area of the PD, g_f and g_c are the optical filter and concentrator gain respectively. Further, L_m denotes the Lambertian order [19].

The SINR $\zeta_{i,j}^{WiFi}$ between user i and WiFi AP j is calculated as [19]:

$$\zeta_{ij}^{WiFi} = \frac{G_{ij}^{WiFi} P_{WiFi}}{N_{WiFi} U_{ij} + \sum_{\substack{w_\alpha \in w_j \\ \alpha \neq j}} \left(G_{ij}^{WiFi} P_{WiFi} \right)}, \tag{24}$$

where P_{WiFi} and N_{WiFi} are WiFi AP's transmit power and noise power spectral density, respectively.

The channel capacity of user i from AP j per RU can be calculated as [8]:

$$H_{ij}^{0} = \eta_{ij} W_j, \tag{25}$$

where, η_{ij} represents the spectral efficiency of user i connected to AP j, determined through adaptive modulation and coding scheme (AMCS) based on the SINR values [35], and W_j is the amount of bandwidth per RU.

The channel gain is expressed as [19]:

$$G_{ij}^{WiFi} = \left| I_{ij}^{WiFi} \right|^2 10^{-\frac{PL(d_{ij})}{10}}, \tag{26}$$

where I_{ij}^{WiFi} is the WiFi channel response and $PL(d_{ij})$ is pathloss of the WiFi multipath propagation model [19].

When the user receives the data from both LiFi and WiFi APs, there is an effect of overhead on the total data, i.e. the total data is limited to β times the sum. We consider the value of β as 0.8 as reported in prior implementations [16] i.e. 80% of the packets are aggregated successfully. The simulation parameters for the above indoor environment for LiFi and WiFi channels are listed in Table II.

B. Performance Evaluation of FLADA

We first compare the performance of FLADA with the ILP and a few baseline techniques. The baseline technique Greedy always uses the maximum data rate possible from the AP nearest to it. The baseline technique Base-FLADA utilizes only Algorithm 1, but not Algorithms 2-3 so that it uses only the LP-rounding approach without any reallocation of the released data rates. In each of the experiments, we choose the location of the users randomly with uniform distribution a total of 200 times, and then report the statistics as box plots.

1) Comparison of Sum Rates Obtained using FLADA: Fig. 6(a) compares the sum rate using a box plot for the techniques Greedy, Base-FLADA and ILP for the specified network along with FLADA for a total 10 number of users. Note that FLADA theoretically only guarantees a sum rate that is not less than 50% of the optimal. In practice, FLADA performs much better in practice on average than its worst-case result, with the median being 82%, 79% and 66% of the median optimal ILP for γ values of 0.1, 0.5 and 0.9 respectively.

We also observe that the achieved sum rate falls with an increase of the fairness coefficient γ. This is expected, as we have a hard fairness constraint, which leads to the release of additional data rates in Algorithm 3. However, the performance of the greedy algorithm falls much more drastically than that of FLADA or ILP. This is because the greedy algorithm does not consider the data rate received by other users at all while doing the first allocation, making its initial allocation more unfair. Thus, FLADA provides much higher data rates than Greedy in terms of percentage at higher values of γ. Likewise, we evaluated the effectiveness of our proposed FLADA without reallocation, referred to as Base-FLADA. The results unveiled a significant decrease in the sum rate when compared to the optimal FLADA. This reduction can be attributed to the fact that a significant amount of additional allocation occurs due to the utilization of Algorithms 2-3.

We further observe the approximation ratios obtained by taking the ratio of FLADA and ILP for each instance of the problem (shown in Fig. 7). As expected, in all cases, the approximation ratio is over 0.5. In general, the median ratio is 0.82, 0.79 and 0.66 for γ values of 0.1, 0.5 and 0.9 respectively. This confirms the statement of Theorem 3, i.e. FLADA always provides $\geqslant 0.5\times$ the optimal result.

2) Effect of Blockage on Sum Rate: In this paper, we address the phenomenon of human blockage within a confined indoor space measuring $5m \times 5m \times 3m$. Following the modeling framework established in literature [36], we represent human blockages within this environment. Specifically, for each user within the system, we consider the presence of $(m-1)$ human blockages, where m corresponds to the total number of users. To characterize the channel impulse response between user i and access point j in the presence of blockages, we employ the following expression:

$$I_B = I_{ij}[1 - P(B)], \tag{27}$$

where $P(B)$ denotes the probability of encountering blockages. To effectively model human blockages, we leverage Matérn hard-core point processes (MHCP), a well-established approach in the literature [36].

We examine the impact of blockages on the system's overall performance by comparing the sum rate under different fairness coefficients. We find that under the unfair allocation scenario $\gamma = 0.1$, we observe negligible impact from blockages on the sum rate. However, as fairness increases $\gamma = 0.5$ and 0.9, the sum rate experiences a noticeable decline in the presence of blockages compared to a blockage-free network.

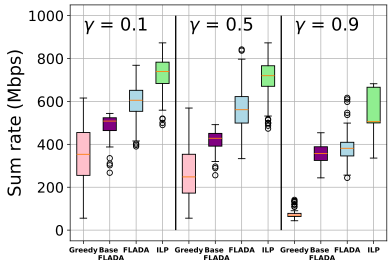

(a)

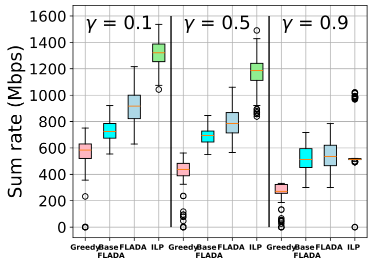

(b)

Fig. 6: Comparisons of sum rate for proposed FLADA with the baselines greedy search, proposed no-reallocated based FLADA (Base-FLADA) and optimal ILP case for various fairness coefficient values for two scenarios: (a) four LiFi APs and single WiFi AP in a small room of $5 \times 5 \times 3m^3$ dimension, and (b) twelve LiFi APs and three WiFi APs in a large room of dimension $15 \times 5 \times 3m^3$.

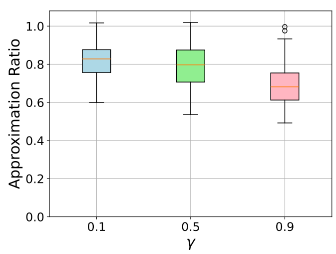

Fig. 7: Comparisons of approximation ratio for different fairness coefficients for FLADA which provides a minimum of 0.5, as proven by Theorem 3 (§IV C).

Furthermore, our FLADA technique demonstrates significant performance enhancements, achieving a 14 % and 24 % improvement in the sum rate under blockage-free conditions compared to scenarios with blockages for γ = 0.5 and 0.9, respectively, within the Hybrid LiFi/WiFi Network (HLWN), as illustrated in Fig. 9.

3) Comparison of Sum Rates Obtained using FLADA in a large setup: Fig. 6(b) compares the sum rate using a box plot for the techniques Greedy, Base-FLADA, and ILP for the specified network, along with FLADA for a total 30 number of users in a room of dimension $15 \times 5 \times 3m^3$. We have considered 12 LiFi APs and 3 WiFi APs to evaluate the sum rate. In practice, FLADA performs much better on average than its worst-case result, with the median being 69%, 66%, and 96% of the median optimal ILP for γ values of 0.1, 0.5, and 0.9 respectively as illustrated in Fig. 6.

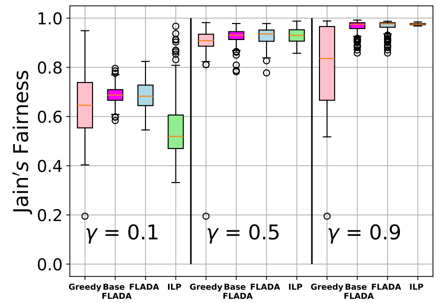

Fig. 8: Jain's fairness index for different values of fairness coefficient.

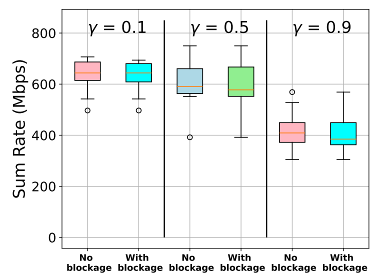

Fig. 9: Comparison of sum rate for proposed FLADA in the presence of blockage and no blockage scenarios in case of data rate allocated to users over LiFi channel.

4) Jain's Fairness: Jain's fairness is evaluated for the proposed FLADA algorithm for different fairness coefficient values as depicted in Fig. 8 for m = 10. Jain's fairness evaluation for a ten-user system shows that the baseline Greedy approach and Base-FLADA perform approximately similarly to the proposed FLADA for $\gamma = 0.1$ due to a less fair network. With an increase in the value of γ, FLADA performs better in Jain's fairness evaluation metric than the baseline. Because the network becomes fairer with the increase in γ. For $\gamma = 0.5$, Jain's fairness follows the same trend as $\gamma = 0.1$; but Jain's fairness is nearly the same for all the approaches. The reason is that fairness is already being considered in the evaluation of the throughput of the network. However, with an increase in γ to 0.9, the proposed FLADA performs better than the baseline greedy approach. We observe that there is a trade-off between average throughput and fairness. Therefore, Jain's fairness decreases while the sum rate increases in FLADA, greedy, Base-FLADA, and ILP as illustrated in Fig. 6.

5) Run Time: : The run time for the proposed FLADA and ILP is illustrated in Fig.10 for small as well as large room dimensions. The system's configuration is AMD Ryzen 5 3600 6-Core Processor @ 3.8 GHz and 16 GB RAM. We observe that the proposed solution takes a maximum of 3.92 ms, while ILP takes a maximum of 0.136 seconds in a single room. For the larger hall, FLADA still takes a maximum of around $50ms$, whereas an ILP even takes as much as 1 minute. Thus, FLADA is around $35\times$ faster than ILP in the single room, and over $1200\times$ faster in the larger room. Furthermore, ILP has large variations that even exceeds $10s$ of run time for larger dimensions of rooms with more users, LiFi, and WiFi APs.

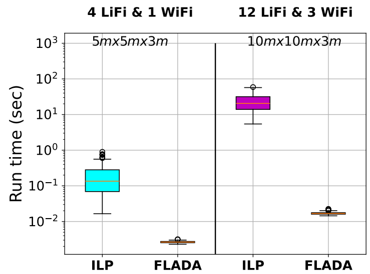

Fig. 10: Comparison of run time for FLADA and ILP in small and large room dimensions.

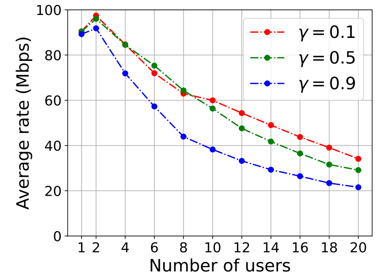

Fig. 12: Average achieved rate for various numbers of users by using FLADA for HLWN with link aggregation.

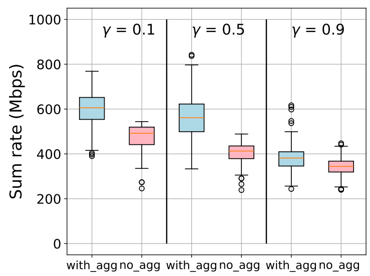

Fig. 11: Sum rate comparisons for FLADA with link aggregation and without link aggregation enabled HLWN network for various fairness coefficient values.

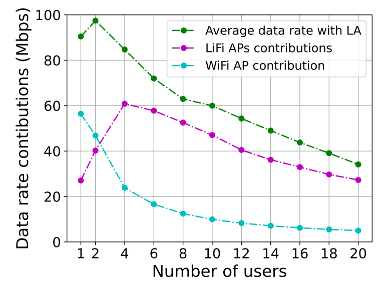

Fig. 13: Contributions of LiFi APs and WiFi APs for the LA-enable network for various number of users.

FLADA has very little variation in the run time, making it more reliable to use in practice.

C. Detailed Performance Analysis of FLADA

We now show a more detailed analysis of FLADA by analyzing its behavior in different situations. These include its utilization of aggregation, its individual data rates for different number of users, the contribution of LiFi and WiFi individually, overall user satisfaction ratios, and energy efficiency.

1) Performance of Link Aggregation: We further show the sum rate of the HLWN with and without aggregation for different values fairness coefficients in Fig. 11. We observe that there is an improvement of the sum rate of approximately 149 Mbps for $\gamma = 0.5$ and $m = 10$ in the case of link aggregation-enabled HLWN than the case without link aggregation. Similarly, we notice that HLWN also performs better by enabling link aggregation than without enabling link aggregation for $\gamma = 0.1$ and $\gamma = 0.9$.

2) Effect of Varying Number of Users: We compare the average achieved data rate by varying the number of users from $m = 1$ to 20 for FLADA for various fairness coefficients as shown in Fig. 12. We observe that from $m = 2$ to 20, there is a consistent fall in the average data rates achieved. This is expected, as both channel and backhaul capacity remain constant. Only from $m = 1$ to $m = 2$, the average data rate increases slightly as the channel capacity is not a constraint for such few number of users with less fair case. Furthermore, the fairness constraint has a limited role in affecting the data rate for a low (< 2) number of users, as it is possible to provide a high enough data rate to satisfy almost all the users.

We notice that the average data rate variations remain same for $\gamma = 0.1$ and 0.5 upto $m = 8$; i.e., there is no effect of the fairness for less number of users. The average data rate is higher in case of $\gamma = 0.1$ than with $\gamma = 0.5$ for $m = 9$ to 20, as some of the users get very high data rate and some gets very low data rate in case of $\gamma = 0.1$ than with $\gamma = 0.5$. Furthermore, strict fairness of $\gamma = 0.9$ provides lower average data rate as compared to other fairness values.

3) Contribution of LiFi and WiFi APs: Fig. 13 illustrates the contributions of the APs towards the achieved data rate of the users. We observe that the average achieved rate depends on the LiFi and WiFi APs contributions. The LiFi APs and WiFi APs serve multiple users based on the available capacity of APs. With an increase in the number of users, the available capacity reduces, and the contribution to the achieved data rates of the APs decreases. In the case of a lower number of users (< 4), the contribution of LiFi APs increases upto four number of LiFi APs, which is obvious. The average data rate obtained by each r_i^0 lies at around $0.97\times$ the summation of data rates received from LiFi and WiFi APs (denoted by $g_{wi}^0 + g_{li}^0$). Note that the data rate must lie between $\beta\times$ and $1\times$ the summation, due to the overhead. Thus, the amount of data rate lost to overhead is only 0.03 times the summation. This small amount of overhead incurred in practice suggests that our algorithm performs better, as it is largely able to avoid the overhead of aggregation by intelligent data rate allocation.

4) Study of User Satisfaction: The user's satisfaction S is defined as the ratio of the achieved data rate by the user to the user's demand, i.e. $S = r_i^0/R_i$. The complementary cumulative distribution function (CCDF) of the user's satisfaction is shown in Fig. 14. Here, the requested data rate is Poisson distributed with mean (λ) of 100 Mbps [37] and $m = 10$. The

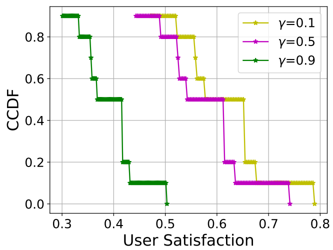

Fig. 14: Analysis of user satisfaction for LA-enabled HLWN for different fairness coefficient values.

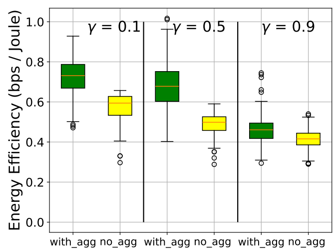

Fig. 15: Efficiency in terms of the maximum total number of bits that the heterogeneous LiFi-WiFi network can deliver per Joule of energy with and without aggregation.

capacity b_j of each LiFi and for WiFi are 200 Mbps and 100 Mbps, respectively.

The user satisfaction for $\gamma = 0.1$ has large deviations as compared to $\gamma = 0.5$ and 0.9 cases. This is because there is a trade-off between fairness and user satisfaction. For $\gamma = 0.5$, user satisfaction has a maximum value of 0.73. Note that the sum of user demand is around 1000 Mbps, whereas the total backhaul capacity equals 900 Mbps. This implies that the best possible user satisfaction equals $900/1000 = 0.9$. Thus, the user satisfaction achieved by our algorithm FLADA is close to the best possible value for lower fairness, i.e., $\gamma = 0.1$. However, user satisfaction is sacrificed for a more fair network, i.e., for $\gamma = 0.5$ and 0.9.

5) Energy-efficiency of Link Aggregation: Fig. 15 depicts the network efficiency measured as the maximum number of bits that can be received per joule of energy at the user end. We consider the cases both with and without aggregation in a heterogeneous LiFi-WiFi network. Note that both WiFi and LiFi APs have significant static power that is consumed even if no data communication is performed. We observe that aggregation enables higher energy efficiency than the case of no aggregation. This is because aggregation enables us to re-utilize the static energy (as per Table II) that is already being spent by the APs for data communication.

VII. Conclusion

In this work, we proposed an algorithm FLADA to maximize the sum of data rates across all the users for LA-enabled heterogeneous LiFi and WiFi network. FLADA satisfies the required fairness constraints, while also handling the data availability based on SINR and the backhaul capacity of APs. We first proved that the problem of maximizing the data rate in such a setting is NP-Hard. Thus, FLADA works by using an LP-Rounding technique, followed by a series of steps involving reallocation and release of data rates. We compare the performance of FLADA to an optimal case of ILP with the baselines greedy approach and Base-FLADA. We observed that FLADA provides 82% of the optimal solution given by ILP while also outperforming the baseline greedy approach and Base-FLADA by 81.6% and 64% for most faired case, respectively. For future work, we plan to improve energy efficiency by performing better power allocation, as well as consider mobility in the system.

References

[1] T. Cogalan and H. Haas, "Why would 5G need optical wireless communications?" in *IEEE 28th Annual International Symposium on Personal, Indoor, and Mobile Radio Communications (PIMRC)*, 2017, pp. 1–6.

[2] G. Ma, R. Parthiban *et al.*, "An adaptive handover scheme for hybrid LiFi and WiFi networks," *IEEE Access*, vol. 10, pp. 18 955–18 965, 2022.

[3] X. Wu, M. D. Soltani *et al.*, "Hybrid LiFi and WiFi networks: A survey," *IEEE Communications Surveys and Tutorials*, vol. 23, no. 2, pp. 1398–1420, 2021.

[4] Y. Wang, X. Wu *et al.*, "Load balancing game with shadowing effect for indoor hybrid LiFi/RF networks," *IEEE Transactions on Wireless Communications*, vol. 16, no. 4, pp. 2366–2378, 2017.

[5] F. Jin, R. Zhang *et al.*, "Resource allocation under delay-guarantee constraints for heterogeneous visible-light and RF femtocell," *IEEE Transactions on Wireless Communications*, vol. 14, no. 2, pp. 1020–1034, 2014.

[6] M. Kashef, M. Ismail *et al.*, "Energy efficient resource allocation for mixed RF/VLC heterogeneous wireless networks," *IEEE Journal on Selected Areas in Communications*, vol. 34, no. 4, pp. 883–893, 2016.

[7] R. Ahmad, M. D. Soltani *et al.*, "Reinforcement learning-based near-optimal load balancing for heterogeneous LiFi WiFi network," *IEEE Systems Journal*, vol. 16, no. 2, pp. 3084–3095, 2022.

[8] R. Ahmad and A. Srivastava, "Sequential load balancing for link aggregation enabled heterogeneous LiFi WiFi network," *IEEE Open Journal of Vehicular Technology*, vol. 3, pp. 138–148, 2022.

[9] C. Deng, X. Fang *et al.*, "IEEE 802.11be Wi-Fi 7: New challenges and opportunities," *IEEE Communications Surveys & Tutorials*, vol. 22, no. 4, pp. 2136–2166, 2020.

[10] A. Potapov and M. Ali, "Convergence of reinforcement learning algorithms and acceleration of learning," *Physical Review E*, vol. 67, no. 2, p. 026706, 2003.

[11] P. H. Pathak, X. Feng *et al.*, "Visible light communication, networking, and sensing: A survey, potential and challenges," *IEEE Communications Surveys and Tutorials*, vol. 17, no. 4, pp. 2047–2077, 2015.

[12] C. Cheng, "A approximation algorithm to solve the maximum multicommodity flow problem with local dominant," in *3rd International Conference on Electronic Information Technology and Computer Engineering (EITCE)*, 2019, pp. 988–992.

[13] A. F. Zantuti, "Linear capacity algorithms for multicommodity flow problems in computer wan," in *25th International Conference on Systems Engineering (ICSEng)*, 2017, pp. 263–267.

[14] A. Moitra, "Approximation algorithms for multicommodity-type problems with guarantees independent of the graph size," in *50th Annual IEEE Symposium on Foundations of Computer Science*, 2009, pp. 3–12.

[15] M. R. Garey and D. S. Johnson, *Computers and Intractability: A Guide to the Theory of NP-Completeness (Series of Books in the Mathematical Sciences)*. W. H. Freeman, 1979.

[16] C. Zeng and S. Licardie, "Systems and methods for performing layer one link aggregation over wireless links," Sep. 1 2015, uS Patent 9,125,084.

[17] Y. Wang and H. Haas, "Dynamic load balancing with handover in hybrid Li-Fi and Wi-Fi networks," *Journal of Light-wave Technology*, vol. 33, no. 22, pp. 4671–4682, 2015.

[18] X. Li, R. Zhang *et al.*, "Cooperative load balancing in hybrid visible light communications and WiFi," *IEEE Transactions on Communications*, vol. 63, no. 4, pp. 1319–1329, 2015.

[19] X. Wu, M. Safari *et al.*, "Access point selection for hybrid Li-Fi and Wi-Fi networks," *IEEE Transactions on Communications*, vol. 65, no. 12, pp. 5375–5385, 2017.

[20] M. Ayyash, H. Elgala *et al.*, "Coexistence of WiFi and LiFi toward 5G: concepts, opportunities, and challenges," *IEEE Communications Magazine*, vol. 54, no. 2, pp. 64–71, 2016.

[21] W. Zhang, L. Chen *et al.*, "Design and realization of indoor VLC-Wi-Fi hybrid network," *Journal of Communications and Information Networks*, vol. 2, no. 4, pp. 75–87, 2017.

[22] A. Zubow, P. Gawowicz *et al.*, "Hybrid-Fidelity: Utilizing IEEE 802.11 MIMO for practical aggregation of LiFi and WiFi," *IEEE Transactions on Mobile Computing*, pp. 1–1, 2022.

[23] S. Shao, A. Khreishah *et al.*, "Design and analysis of a visible-light-communication enhanced WiFi system," *Journal of Optical Communications and Networking*, vol. 7, no. 10, pp. 960–973, 2015.

[24] Y. S. M. Pratama and K. W. Choi, "Bandwidth aggregation protocol and throughput-optimal scheduler for hybrid RF and visible light communication systems," *IEEE Access*, vol. 6, pp. 32 173–32 187, 2018.

[25] A. Zubow, P. Gawłowicz *et al.*, "Hy-Fi: Aggregation of LiFi and WiFi using MIMO in IEEE 802.11," in *22nd International Symposium on a World of Wireless, Mobile and Multimedia Networks (WoWMoM)*, 2021, pp. 100–108.

[26] W. Wu, F. Zhou *et al.*, "Adaptive network resource optimization for heterogeneous vlc/rf wireless networks," *IEEE Transactions on Communications*, vol. 66, no. 11, pp. 5568–5581, 2018.

[27] H. Yang, A. Alphones *et al.*, "Learning-based energy-efficient resource management by heterogeneous rf/vlc for ultra-reliable low-latency industrial iot networks," *IEEE Transactions on Industrial Informatics*, vol. 16, no. 8, pp. 5565–5576, 2020.

[28] J. Kong, Z.-Y. Wu *et al.*, "Q-learning based two-timescale power allocation for multi-homing hybrid rf/vlc networks," *IEEE Wireless Communications Letters*, vol. 9, no. 4, pp. 443–447, 2020.

[29] N. M. Karoti, S. Paramita *et al.*, "Improving the performance of heterogeneous LiFi-WiFi network using a novel link aggregation framework," in *2022 IEEE Wireless Communications and Networking Conference (WCNC)*, 2022, pp. 2322–2327.

[30] J. Ghimire and C. Rosenberg, "Resource allocation, transmission coordination and user association in heterogeneous networks: A flow-based unified approach," *IEEE Transactions on Wireless Communications*, vol. 12, no. 3, pp. 1340–1351, 2013.

[31] F. Wang, W. Chen *et al.*, "Joint optimization of user association, subchannel allocation, and power allocation in multi-cell multi-association OFDMA heterogeneous networks," *IEEE Transactions on Communications*, vol. 65, no. 6, pp. 2672–2684, 2017.

[32] Y. Chen, J. Li *et al.*, "Joint user association and resource allocation in the downlink of heterogeneous networks," *IEEE Transactions on Vehicular Technology*, vol. 65, no. 7, pp. 5701–5706, 2016.

[33] S. Gopalam, S. V. Hanly *et al.*, "Distributed user association and resource allocation algorithms for three tier HetNets," *IEEE Transactions on Wireless Communications*, vol. 19, no. 12, pp. 7913–7926, 2020.

[34] X. Ge, L. Pan *et al.*, "Wireless backhaul capacity of 5g ultra-dense cellular networks," in *IEEE 84th Vehicular Technology Conference (VTC-Fall)*, 2016, pp. 1–6.

[35] "Minimum 802.11 SNR Sensitivity — antennas and accessories." [Online]. Available: https://interline.pl/Information-and-Tips/Minimum-802.11-SNR-Sensitivity

[36] A. Singh, G. Ghatak *et al.*, "Performance analysis of indoor communication system using off-the-shelf leds with human blockages," *IEEE Open Journal of the Communications Society*, vol. 2, pp. 187–198, 2021.

[37] A. Ichigaya and Y. Nishida, "Required bit rates analysis for a new broadcasting service using hevc/h. 265," *IEEE Transactions on Broadcasting*, vol. 62, no. 2, pp. 417–425, 2016.